Cellular and Molecular Life Sciences (2021) 78:1113–1129
https://doi.org/10.1007/s00018-020-03568-x

ORIGINAL ARTICLE

The proteostasis guardian HSF1 directs the transcription of its paralog and interactor HSF2 during proteasome dysfunction

Silvia Santopolo[1] · Anna Riccio[1] · Antonio Rossi[2] · M. Gabriella Santoro[1,2]

Received: 30 December 2019 / Revised: 3 May 2020 / Accepted: 28 May 2020 / Published online: 30 June 2020

Abstract

Protein homeostasis is essential for life in eukaryotes. Organisms respond to proteotoxic stress by activating heat shock transcription factors (HSFs), which play important roles in cytoprotection, longevity and development. Of six human HSFs, HSF1 acts as a proteostasis guardian regulating stress-induced transcriptional responses, whereas HSF2 has a critical role in development, in particular of brain and reproductive organs. Unlike HSF1, that is a stable protein constitutively expressed, HSF2 is a labile protein and its expression varies in different tissues; however, the mechanisms regulating HSF2 expression remain poorly understood. Herein we demonstrate that the proteasome inhibitor anticancer drug bortezomib (Velcade), at clinically relevant concentrations, triggers de novo HSF2 mRNA transcription in different types of cancers via HSF1 activation. Similar results were obtained with next-generation proteasome inhibitors ixazomib and carfilzomib, indicating that induction of HSF2 expression is a general response to proteasome dysfunction. HSF2-promoter analysis, electrophoretic mobility shift assays, and chromatin immunoprecipitation studies unexpectedly revealed that HSF1 is recruited to a heat shock element located at 1.397 bp upstream from the transcription start site in the HSF2-promoter. More importantly, we found that HSF1 is critical for HSF2 gene transcription during proteasome dysfunction, representing an interesting example of transcription factor involved in controlling the expression of members of the same family. Moreover, bortezomib-induced HSF2 was found to localize in the nucleus, interact with HSF1, and participate in bortezomib-mediated control of cancer cell migration. The results shed light on HSF2-expression regulation, revealing a novel level of HSF1/HSF2 interplay that may lead to advances in pharmacological modulation of these fundamental transcription factors.

Keywords Anticancer · Bortezomib · Cell migration · HSF1 · HSF2 · Proteasome inhibition · Transcriptional regulation

Introduction

Proteome homeostasis, or proteostasis, a finely regulated multi-compartmental process that coordinates protein synthesis, folding and degradation [1], is fundamental for cell health. The 26S-proteasome, a multicatalytic ATP-dependent proteolytic machine consisting of a 19S-regulatory particle and a 20S-core particle with proteolytic activity [2], represents the primary site for non-lysosomal protein degradation in mammalian cells. As part of the ubiquitin–proteasome system (UPS), the proteasome regulates the turnover and quality control of proteins, consequently affecting many aspects of cell physiology, including cell proliferation and differentiation, apoptosis and signal transduction [3, 4]. Because of its central role in protein homeostasis, the 26S-proteasome is considered an attractive target in anticancer therapy due to increased protein metabolism in tumor cells, and a variety of heterogeneous reversible and irreversible proteasome inhibitors (PI) have been identified [5–7]. Among these, the reversibly binding dipeptide boronate-based bortezomib (Velcade, formerly PS-341) represents the first-in-class PI used in the clinic for treatment of multiple myeloma (MM) and relapsed mantle cell lymphoma [8], and is known to possess anticancer activity against several other malignancies based on its direct pro-apoptotic effects on cancer cells as well as its antiangiogenic action [9, 10].

Electronic supplementary material The online version of this article (https://doi.org/10.1007/s00018-020-03568-x) contains supplementary material, which is available to authorized users.

✉ M. Gabriella Santoro
santoro@uniroma2.it

[1] Department of Biology, University of Rome Tor Vergata, Via della Ricerca Scientifica, 00133 Rome, Italy

[2] Institute of Translational Pharmacology, CNR, Rome, Italy

Next-generation PI, including the irreversibly binding peptide epoxyketone-based carfilzomib and the orally available boronate-based ixazomib, have been developed to overcome intrinsic or acquired resistance, as well as off-target toxicity of bortezomib [11].

A critical consequence of the ubiquitin–proteasome network down-regulation is the activation of the cellular heat shock response (HSR) [12]. Following its seminal discovery in *Drosophila* by Ferruccio Ritossa in the early 1960s [13], the HSR, also known as proteotoxic stress response, is recognized as a fundamental highly conserved mechanism evolved from yeast to humans to protect cells from the damaging effects of proteostasis disruption by triggering the expression of cytoprotective heat shock proteins (HSP) [14]. HSPs, which include members of the HSP70 and HSP90 families, HSP27 and other proteins of the network, act as molecular chaperones that maintain cellular proteostasis through facilitation of folding, transport, ubiquitination, and proteasomal degradation of proteins [12, 14].

The HSR is regulated by a family of heat shock (HS) transcription factors (HSFs) that are expressed and maintained in an inactive state under non-stress conditions. The human genome encodes six heat shock factors: HSF1, HSF2, HSF4, HSF5, HSFX and HSFY that have different functions and exhibit different and tissue-specific patterns of expression [15]. Among the different HSFs, HSF1 is considered to be the paralog responsible for regulating acute and severe proteotoxic stress-driven transcriptional responses, including exposures to elevated temperatures [16]; although it lacks intrinsic stress-responsiveness HSF2, that exists in two alternative-splicing isoforms (α and β) [17], also contributes to inducible expression of HS genes through interplay with HSF1, acting as a fine tuner of the HSR [18–21].

HSF1 and HSF2 are multi-domain transcription factors both containing an amino-terminal DNA-binding domain, an adjacent multimerization domain, a central regulatory domain, a carboxyl-terminal coiled-coil domain and a transcriptional activation domain [17]. HSF1 is generally found as an inert monomer in unstressed cells; upon exposure to proteotoxic stress, HSF1 is derepressed in a stepwise process that involves trimerization, nuclear translocation, phosphorylation/sumoylation, and binding to DNA sequences (heat shock elements, HSE); functional HSE sequences are characterized by an array of inverted repeats of the pentameric motif -nGAAn-, which are usually located in the proximal region of HSF1-responsive gene promoters, but may vary in sequence and geometry in different target genes [16, 22]. In human cells, beyond HS genes, HSF1-binding sites have been described in a broad repertoire of genes encoding proteins with non-chaperone function [23–25].

HSF2 DNA-binding domains are closely related to HSF1-binding motifs, although the two factors are known to exhibit slight differences in HSE recognition and occupancy [26], and display distinct regulatory interactions [27, 28]. Opposite to HSF1, HSF2 is not effective in activating the HSR under stress conditions and is, in fact, rapidly degraded by the proteasome during heat shock [29, 30]. HSF2 is instead mainly expressed during development and differentiation, in particular of brain and reproductive organs, and is recognized as a critical factor in brain development [31–33]; as a consequence, HSF2 deficiency has been linked to embryonic and adult brain defects associated with central nervous system abnormalities [34, 35], and reduced size of testes together with decreased sperm count; specific mutations in HSF2 have been associated with idiopathic azoospermia [36–38]. In addition, an important role of HSF2 in erythroid differentiation has been shown in hemin-directed differentiation studies [39].

Despite their similarity in the overall domain structure, a major difference between HSF1 and HSF2 is their relative stability: HSF1 is a stable protein evenly and constitutively expressed, whereas HSF2 is a short-lived protein and its levels vary in different types of tissues and may fluctuate during the cell cycle as well as in developmental processes [21, 27, 40]. HSF2 expression appears to be finely regulated both at the transcriptional and post-translational level; however, the mechanisms involved remain poorly understood. Differently from HSF1, whose activity is mainly regulated by post-translational modifications (phosphorylation, sumoylation and acetylation) [15], it has been proposed that HSF2 activity may depend on its intracellular level [30, 41]. In unstressed conditions HSF2 mainly exists as an inactive dimer [15, 28], and the mere increase in its concentration was shown to cause HSF2 translocation into the nucleus and binding to DNA after forming homotrimers or heterotrimers with HSF1 [18, 31, 42]; several studies have in fact revealed direct physical and functional interactions between HSF1 and HSF2 [18, 20, 28].

In the case of cancer, HSF1 has been found to be highly expressed and constitutively localized into the nucleus of different types of cancer cells, and it has been associated with higher proliferation potential and increased cell survival [43–46]. On the other hand, very little is known on the role of HSF2 in cancer.

We have recently reported that treatment with the PI bortezomib causes an increase in HSF2 RNA and protein levels in human primary cells [20]. Whereas it was expected that proteasome inhibition would lead to HSF2 protein stabilization/accumulation, this was not the case for HSF2 mRNA, and suggested that the anticancer drug may regulate HSF2 expression at the transcriptional or post-transcriptional level. We now demonstrate that bortezomib, at clinically relevant concentrations, induces de novo HSF2 transcription in human cancer cells. Analysis of the human HSF2 promoter, electrophoretic mobility shift and supershift assays, and chromatin immunoprecipitation studies reveal that HSF1

is recruited to the HSF2 promoter after bortezomib treatment in cancer cells. The binding sequence, located at 1.397 bp upstream from the transcription start site, was identified. Surprisingly, we found that HSF1 plays a fundamental role in promoting the expression of its paralog HSF2 during proteasome inhibition. Furthermore, silencing experiments reveal that HSF2 is implicated in bortezomib-mediated control of breast and cervical carcinoma cell migration.

Materials and methods

Cell culture, treatments, plasmids and transfections

Human MDA-MB-231 and MCF7 breast carcinoma (ATCC), HeLa cervical carcinoma (ATCC), KMM-1 multiple myeloma (a kind gift of R. Piva, University of Turin, Italy) and M10 malignant melanoma cells derived from metastatic nodules (kindly provided by G. Zupi, Regina Elena Cancer Institute, Rome, Italy) were grown in DMEM (MDA-MB-231, MCF7 and HeLa) or RPMI-1640 (KMM-1 and M10) medium supplemented with 10% FCS, 2 mM glutamine and antibiotics at 37 °C with 5% CO_2. Cell viability was determined by vital-dye exclusion assay (Trypan blue, 0.1%), as described [47]. Bortezomib, ixazomib-citrate and carfilzomib (Selleckchem) were dissolved in dimethylsulfoxide (DMSO) and diluted in culture medium immediately before use. Bortezomib was used at the concentration of 25 nM, unless differently specified. Actinomycin D (Sigma-Aldrich), dissolved in DMSO, was added to culture medium 45 min before bortezomib treatment. Control media contained the same amount of DMSO-vehicle (< 0.1%). Flag-HSF1-pcDNA3 expression vector was kindly provided by S. Calderwood, Harvard Medical School [48]. Transfections were performed using jetPRIME Transfection Reagent (Polyplus-transfection), according to the manufacturer's instructions.

Recombinant retroviral vectors and generation of stable HSF1-silenced cell lines

Procedures for preparation of siRNAs-coding constructs and for generation of HeLa cells stably transfected with pSUPER-HSF1i (HeLa-HSF1i) or control vector (HeLa-WT) were described previously [49]. For generation of MDA-MB-231, M10 and MCF7 cell lines stably silenced for HSF1 (HSF1i) and their controls (WT), the RNAi-pSUPER-retro vector, containing a puromycin resistance gene for selection of stable transfectants, was used [50]; the human HSF1 gene sequence selected was reported previously [49]. Retroviruses were produced by transfection of 293T cells with plasmids expressing retroviral proteins Gag-Pol, G (VSV-G pseudotype), pSUPER-retro and HSF1i-pSUPER-retro constructs using Lipofectamine 2000 (Invitrogen). At 48 h after transfection, supernatants containing the retroviral particles were collected and frozen at − 70 °C until use. Cells were infected with diluted supernatant in the presence of 8 μg/ml Polybrene overnight, and then selected with puromycin (1 μg/ml) 48 h after infection. After 10 days in selective medium, different pools [HSF1i and control (WT)] for each cell line were isolated. Selected pools were cultured in DMEM (MDA-MB-231 and MCF7) or RPMI-1640 (M10) medium supplemented with puromycin (0.5 μg/ml). The puromycin selective pressure was removed 24 h before experimental procedures.

siRNA interference

Two siRNA duplex target sequences [5′-CCCAAGTAC TTCAAGCACA-3′ (siHSF1-1) and 5′-CAGTGACCACTT GGATGCTAT-3′ (siHSF1-2)] and their scrambled control (scrRNA) (QIAGEN) were used for HSF1-silencing. The siRNA target sequence used for HSF2-silencing was as follows: 5′-GTAGGACTGAAGGTTTAAA-3′ [20]. Transfections were performed using jetPRIME Transfection Reagent, according to the manufacturer's instructions. In brief, cells were plated on 35-mm wells (2×10^5 cells per well) and, after 24 h, were transfected with 50 nM of the indicated siRNAs (siHSF1-1, siHSF1-2, siHSF2), siRNA pools (25 nM siHSF1-1 + 25 nM siHSF1-2) or scrRNA. After 24 h, cells were washed twice with culture medium and transfection was repeated as above. At 12 h after the second transfection, siRNAs were removed, and cells were washed twice with culture medium before bortezomib treatment.

Western blot analysis

Whole-cell extracts (WCE) were prepared after lysis in high-salt extraction buffer (Buffer-B) [25]. Nuclear and cytoplasmic extracts were prepared as described [51]. Equal amounts of proteins (20 μg) were separated by SDS polyacrylamide gel electrophoresis (PAGE), transferred onto nitrocellulose membranes and incubated with rabbit polyclonal anti-HSF2 (sc-13056, Santa Cruz Biotechnology), anti-HSF1 (sc-9144, Santa Cruz Biotechnology), anti-HSF1 (phospho-S326) (EP1713Y, Abcam), anti-ZFAND2A (HPA019469, Sigma-Aldrich), anti-PARP (sc-7150, Santa Cruz Biotechnology), anti-Flag (2368, Cell Signaling), anti-β-actin (A2066, Sigma-Aldrich) antibodies or monoclonal anti-HSP70 (SPA-810, Stressgen), anti-ubiquitin (sc-8017, Santa Cruz Biotechnology), anti-TBP (ab818, Abcam), anti-α-tubulin (T5168, Sigma-Aldrich) antibodies, followed by decoration with peroxidase-labeled anti-rabbit or anti-mouse IgG, respectively (Super-Signal detection kit, Pierce). All the results shown are representative of at least three independent experiments.

Electrophoretic mobility shift assay (EMSA)

The 35-bp HSP70-HSE DNA probe was described previously [52]. The HSF2-HSE DNA probes containing the HSF-binding sites described in Fig. 4A were 5′-CAACTT TTGAGTCTCAGAATCTTCTCTGGG-3′ (HSF2-HSEa) and 5′-AAAAAAAAAAAGTCGAATTTTGTAGACTTC -3′ (HSF2-HSEb). The mutated HSF2-HSEa probe (HSF2-HSEa mut, Fig. S3B) was 5′-CAACTTTTGAGTCTCA TAATCTTCTCTGGG-3′. WCE (15 µg) prepared after lysis in high-salt extraction buffer were incubated with a ^{32}P-labeled HSE DNA probe [53] followed by analysis of DNA-binding activity by EMSA. Binding reactions were performed as described [51]. Complexes were analyzed by nondenaturing 4% polyacrylamide gel electrophoresis. To determine the specificity of HSF-DNA complexes, WCE were preincubated with different dilutions of anti-HSF1 (sc-9144, Santa Cruz Biotechnology) antibodies for 15 min before electromobility supershift assay [54].

RNA analysis

Total RNA was extracted using the TRIzol reagent (Life Technologies) as described in the manufacturer protocol. Reverse transcription-polymerase chain reaction (RT-PCR) (1 µg RNA) was performed as described [25]. Real-time PCR (qPCR) analysis was performed with CFX96 (Bio-Rad), using SsoAdvanced Universal SYBR Green Supermix (Bio-Rad). Relative quantities of HSF2 and HSP70 RNA were normalized to ribosomal L34 RNA levels. The sequences of the HSP70 primers and the HSF2 primers, amplifying both α and β isoforms, were described previously [20]. The sequences of the L34 primers were as follows: sense 5′-GGCCCTGCTGACATGTTTCTT-3′, antisense 5′-GTCCCGAACCCCTGGTAATAGA-3′. All reactions were made in triplicate using samples derived from at least three biological repeats.

Newly synthesized (NS) RNA was isolated using the Click-iT® Nascent RNA Capture Kit (Life Technologies) following the manufacturer protocol. In brief, NS-RNA was labeled by adding 5-ethynyl uridine (EU) to growing cells. Total RNA, extracted as described above, was used as a template in a click reaction with an azide-modified biotin; RNA was precipitated overnight at − 70 °C by adding 100% ethanol (700 µl), UltraPure glycogen (1 µl) and 7.5 M ammonium acetate (50 µl). NS-RNA was isolated from total RNA using Dynabeads® MyOne™ Streptavidin T1 magnetic beads (Life Technologies) and after extensive washing, was subjected to reverse transcription using SuperScript® VILO cDNA Synthesis Kit (Life Technologies) and quantified by qPCR as described above.

Nuclear *run-on* (NRO) assay was performed as described by Roberts et al. [55]. In brief, cells were harvested and lysed in NP-40 lysis buffer [10 mM Tris–HCl (pH 7.4), 10 mM NaCl, 3 mM $MgCl_2$, 0.5% NP-40], and after centrifugation, nuclear pellets were resuspended in nuclei storage buffer [50 mM Tris–HCl (pH 8.3), 0.1 mM EDTA, 5 mM $MgCl_2$, 40% glycerol]. In vitro run-on transcription in isolated nuclei was performed in the presence of a non-radioactive labeled ribonucleotide precursor (5-Bromouridine 5′-Triphosphate; Sigma-Aldrich) for 30 min at 30 °C. Total RNA was extracted with MEGAClear Transcription Clean-Up Kit (AM1908, Life Technologies) and bromouridylated-NRO-RNA was isolated from total RNA using anti-BrdU monoclonal antibodies (sc-32323, Santa Cruz Biotechnology) and Protein G Dynabeads (10003D, Life Technologies), and extracted using TRIzol reagent. NRO-RNA was subjected to reverse transcription and quantified by qPCR as described above.

All reactions were made in triplicate using samples derived from at least three biological repeats.

In silico HSF2 promoter analysis

The sequence of a 2500-bp region upstream of the transcription start site of the human HSF2 gene has been analyzed by JASPAR 2018 [56] to identify putative heat shock elements (HSE) in the HSF2 promoter. Two putative HSE located at − 1.397 bp (HSEa) and − 1.016 bp (HSEb) upstream of the transcription start site were detected (Fig. 4A, B).

Chromatin Immunoprecipitation (ChIP) assay

ChIP assay was performed as described by Carey et al. [57]. In brief, cross-linking was performed by adding 1% formaldehyde to cell medium for 10 min. After quenching by addition of glycine to a final concentration of 0.137 M, cells were washed with PBS, harvested and lysed with cell lysis buffer [5 mM PIPES (pH 8), 85 mM KCl and 0.5% NP-40]. After centrifugation the pellet was resuspended in nuclei lysis buffer [50 mM Tris–HCl (pH 8), 10 mM EDTA, 1% SDS] supplemented with protease inhibitors. Chromatin was sheared by sonication and precleared for 2 h at 4 °C using protein A-magnetic beads (Bio-Rad). Immunoprecipitation was performed at 4 °C overnight with 5 µg of anti-HSF1 (sc-9144, Santa Cruz Biotechnology) antibodies, or control IgG. After collection with protein A-magnetic beads (Bio-Rad), immunocomplexes were washed four times with high-salt wash buffer [50 mM HEPES (pH 7.9), 500 mM EDTA, 0.1% SDS, 1% Triton X-100, 0.1% deoxycholate], twice with TE buffer [50], and eluted in elution buffer (50 mm Tris–HCl, 10 mM EDTA, 1% SDS) supplemented with Proteinase K (66 µg/ml) for 2 h at 55 °C. Subsequently, the elutes were placed at 65 °C overnight to reverse cross-linking, and the DNA fragments were extracted with phenol:chloroform, precipitated with ethanol using 15 µg of tRNA (Sigma-Aldrich)

as carrier and analyzed by PCR and qPCR as described [50]. The fold enrichment was calculated by comparing the enrichment in the IP samples to the IgG control antibodies, which was arbitrarily set to 1. Sequences of primers amplifying the HSF2 promoter regions were as follows: Region 1 (R1), sense: 5′-CTCCCATTTACTTGCTGTGACTG-3′, antisense: 5′-CCTCACAACAACCCAATGAAC-3′; Region 2 (R2), sense: 5′-ACTTATCCTTGTCACTGCCCTTA-3′, antisense: 5′-CAAATGAGCAATATCACTTATCAGG-3′ (see Fig. 4A for details).

Immunofluorescence microscopy

MDA-MB-231 and HeLa cells grown on coverslips were fixed as described [58] before incubation with rabbit anti-HSF2 antibody (Santa Cruz Biotechnology) for 1 h and incubated with anti-rabbit Alexa Fluor 555 (Thermo Fisher Scientific) for 30 min at room temperature. Nuclei were stained with DAPI. Images were acquired on Olympus Fluoview FV-1000 confocal laser scanning system (Olympus America Inc., Center Valley, PA). Images (resolution, 800 × 800 pixels) were analyzed using Imaris (v6.2) software (Bitplane, Zurich, Switzerland). Three-dimensional (3D) isosurface reconstructions of confocal sections were obtained using Imaris (v6.2) software. Images shown in all figures are representative of at least three random fields.

Proximity ligation assay (PLA)

For PLA-assay, MDA-MB-231 and HeLa cells were grown on coverslips and processed as described in the previous section. After incubation with the primary antibodies, Duolink in situ PLA (Sigma-Aldrich) was performed as described [25]. In brief, PLA probes were incubated for 1 h at 37 °C, followed by hybridization, ligation (30 min at 37 °C) and amplification (100 min at 37 °C). Nuclei were stained with DAPI in Duolink In Situ Mounting Medium (Sigma-Aldrich). The following antibodies were used: monoclonal anti-HSF2 (sc74529, Santa Cruz Biotechnology) and polyclonal anti-HSF1 (sc-9144, Santa Cruz Biotechnology). Images were captured using an Olympus Fluoview FV1000 confocal laser scanning system (Olympus America Inc.) as described above. Images shown in all figures are representative of at least three random fields.

Transwell migration assay

MDA-MB-231 and HeLa cells were silenced for HSF2 and treated with 25 nM bortezomib as described above. The ability of cells to migrate was assessed in a Boyden chamber. Cells were seeded in FBS-free medium, on 8-µm uncoated transwell filters, while media containing 10% FBS were added, as a chemoattractant, to the lower migration chamber. Cells were incubated for 3 or 24 h; non-migratory cells, that had not penetrated the filter, were removed with a cotton-tipped swab. Cells that had migrated to the lower surface of the filter were fixed and stained with a mixture of 6% glutaraldehyde and 0.5% crystal violet for 30 min. Pictures of at least 4 fields per transwell insert (up, down, left, right) were taken under a Leica DM-IL microscope equipped with a 10X objective using a Leica DC300 camera with the Leica-IM500 software. The number of migrated cells in each sample was counted. The experiment was made in triplicate using samples derived from five biological repeats.

Statistical analysis

Statistical analysis was performed using the Student's *t* test for unpaired data or one-way ANOVA test (Prism 5.0 software, GraphPad). Data are expressed as the mean ± SD of samples derived from at least three biological repeats and P values ≤ 0.05 were considered significant. All the results shown are representative of at least three independent experiments, each in duplicate or triplicate.

Results

Proteasome inhibition induces HSF2 expression in cancer cells

Among the different HSFs, HSF2 is characterized as a labile protein whose intracellular levels fluctuate and accumulate following proteasome inhibition [29, 30]. As indicated above, we have recently shown that clinically relevant concentrations of the anticancer PI bortezomib (Fig. 1A), in addition to stabilizing HSF2 protein, also caused an increase in HSF2 mRNA in human primary endothelial cells [20], suggesting that the drug may regulate HSF2 transcription. This observation prompted us to investigate the effect of bortezomib on HSF2 expression in human cancer cells.

In a first set of experiments human multiple myeloma (KMM-1), cervical carcinoma (HeLa), melanoma (M10), luminal-like (MCF7) and mesenchymal-like (MDA-MB-231) breast adenocarcinoma cells were treated with 25 nM bortezomib and, after 14 h, whole-cell extracts (WCE) were analyzed for levels of HSF2, HSF1 and HSP70, as a marker of HSF1 activation, by Western blot, as well as for HSF2 mRNA levels by qPCR. In the absence of treatment, high levels of HSF1 protein were detected in all cell lines tested, whereas HSF2 levels were found to be modest in KMM-1, HeLa, M10 and MCF7 cells and were barely detectable in MDA-MB-231 cells under the conditions analyzed (Fig. 1B, top).

Due to the ubiquitin–proteasome network down-regulation, bortezomib is known to induce HSF1 activation [20];

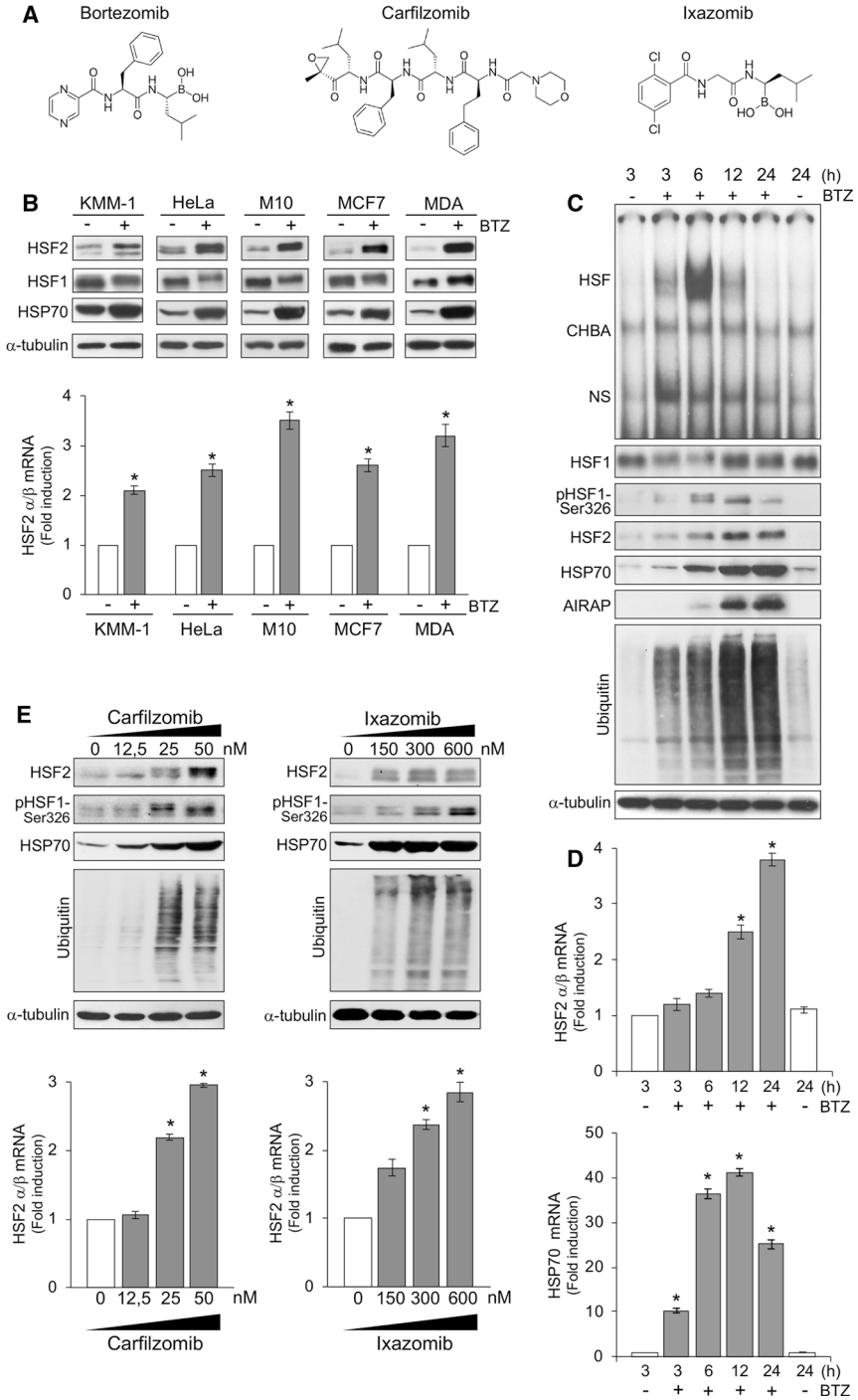

Fig. 1 Proteasome inhibitors induce HSF2 expression in human cancer cells. **A** Structure of proteasome inhibitors bortezomib, carfilzomib and ixazomib. **B** Western blot analysis of HSF2, HSF1, HSP70 and α-tubulin levels in human multiple myeloma (KMM-1), cervical carcinoma (HeLa), melanoma (M10) and breast cancer [MCF7 and MDA-MB-231 (MDA)] cells treated with 25 nM bortezomib (BTZ, +) or vehicle (−) for 14 h (top panels). In parallel samples, HSF2 RNA levels were analyzed by qPCR (bottom panels). **C** Analysis of HSF DNA-binding activity by EMSA in MDA-MB-231 cells at different times after BTZ (25 nM, +) treatment (top panel). Positions of the HSF DNA-binding complex (HSF), constitutive HSE-binding activity (CHBA), and nonspecific protein–DNA interaction (NS) are shown. Levels of HSF1, HSF1-pS326, HSF2, HSP70, AIRAP, polyubiquitinated proteins and α-tubulin were determined in the same samples by Western blot (bottom panels). **D** Total RNA was analyzed for HSF2 (top panel) and HSP70 (bottom panel) RNA by qPCR in samples treated as in **C**. **E** Immunoblot of HSF2, HSF1-pS326, HSP70, polyubiquitinated proteins and α-tubulin levels in MDA-MB-231 cells treated for 14 h with different concentrations of carfilzomib or ixazomib (top panels). In parallel, total RNA was analyzed for HSF2 by qPCR (bottom panels). In **B**, **D** and **E**, relative quantities of HSF2 or HSP70 RNA were normalized to ribosomal L34 RNA levels in the same sample. The fold increase was calculated by comparing the induction of HSF2 or HSP70 in each sample to the relative control (**B**, **E**) or to the control at 3 h (**D**), which were arbitrarily set to 1. All reactions were made in triplicate using samples derived from at least five biological repeats. Error bars indicate mean ± S.D. Students' *t* test (**B**), ANOVA test (**D**, **E**). $^*P < 0.05$

a slight shift in HSF1 molecular weight (a marker of HSF1 phosphorylation), as well as an increase in HSP70 expression, was in fact detected after bortezomib treatment. Parallel to HSP70, bortezomib was found to cause a remarkable increase in HSF2 protein levels in all cancer cell lines (Fig. 1B, top); this effect was particularly evident in MDA-MB-231 cells. Bortezomib-induced HSF2 accumulation could be the result of its stabilization due to proteasome inhibition; however, analysis of KMM-1, HeLa, M10, MCF7 and MDA-MB-231 cell RNA revealed that bortezomib treatment significantly increased HSF2 mRNA level in all cell lines (Fig. 1B, bottom), reinforcing the possibility that the anticancer drug could regulate HSF2 expression also at the transcriptional or post-transcriptional level.

Among the different cell lines analyzed, breast cancer MDA-MB-231 cells were selected as a model to study bortezomib-induced HSF2 expression, based on the marked increase in HSF2 levels induced by the drug in these cells (Fig. 1B). To investigate the kinetics of HSF2 expression, MDA-MB-231 cells were treated with 25 nM bortezomib and, at different times after treatment, WCE were analyzed for levels of HSF2, HSF1, HSP70, the newly identified human HSF1-target AIRAP [24] and polyubiquitinated proteins by Western blot, as well as for HSF1 DNA-binding activity by EMSA; since bortezomib was shown to induce HSF1 phosphorylation on serine 326 [59], the levels of HSF1 pS326 were also analyzed. In parallel samples, total RNA was analyzed for HSF2 and HSP70 by qPCR. As shown in Fig. 1C, bortezomib caused polyubiquitinated proteins accumulation in MDA-MB-231 cells starting at 3 h after treatment, and triggered HSF1 activation, as detected by HSF1 DNA-binding activity and pS326 phosphorylation, as well as by induction of HSP70 and AIRAP expression, starting at 3–6 h after treatment; HSF1 DNA-binding activity was found to attenuate at 24 h after treatment, despite the high level of polyubiquitinated proteins at this time. Bortezomib was found to induce HSF2 expression, both at the mRNA and protein levels, starting at 6 h after treatment (Fig. 1C, D). It should be noted that levels of HSP70 mRNA started to increase earlier than HSF2 mRNA, being already elevated at 3 h after the addition of the drug (Fig. 1D). In addition to bortezomib, elevated HSF2 protein and mRNA levels were detected in MDA-MB-231 cells treated with the next-generation proteasome inhibitors ixazomib and carfilzomib (Fig. 1A, E).

HSF2 predominantly localizes in the nuclei of bortezomib-treated cancer cells and interacts with HSF1

To characterize bortezomib-induced HSF2 intracellular localization, MDA-MB-231 cells were treated with the PI, and after 14 h, nuclear and cytoplasmic fractions were isolated and analyzed by Western blot for HSF2 and HSF1 levels, and for TBP (TATA-binding Protein) and α-tubulin as loading control for nuclear and cytoplasmic fractions, respectively. In parallel, MDA-MB-231 cells growing on coverslips were examined by confocal immunomicroscopy. As shown in Fig. 2A, B, an intense HSF2 immunofluorescent signal, predominantly localized in the nucleus, was detected in treated cells. Consistently with the immunofluorescence, HSF2 was detected only in the nuclear fraction of bortezomib-treated MDA-MB-231 cells when analyzed by Western blot (Fig. 2C). Similar results were obtained in HeLa cells, where high levels of HSF2 were found predominantly in the nuclei 14 h after bortezomib treatment (Fig. S1A), suggesting that HSF2 may participate in bortezomib-regulated transcription in cancer cells.

Since down-regulation of proteasome function is known to induce DNA-binding activity of both HSF1 and HSF2, leading to the formation of HSF1/HSF2 heterotrimeric complexes, HSF1-HSF2 colocalization was detected by in situ proximity ligation assay (PLA) in MDA-MB-231 cells treated with 25 nM bortezomib for 14 h. The results, shown in Fig. 2D, clearly indicate that bortezomib-induced HSF2 interacts with HSF1 in the nuclei of MDA-MB-231 treated cells; the presence of well-defined foci suggests the possibility that HSF2 may interact with HSF1 in selected genomic loci, as previously described [18]. Finally, HSF1–HSF2 interaction was also evident in the nuclei of HeLa cells 14 h after bortezomib treatment (Fig. S1B).

Bortezomib induces de novo HSF2 transcription

To determine whether the increase in HSF2 mRNA levels induced by bortezomib was due to mRNA stabilization or transcription, MDA-MB-231 cells were treated with bortezomib in the presence or the absence of actinomycin D (5 μg/ml) and, after 14 h, HSF2 mRNA and protein levels were analyzed. As shown in Fig. 3A, actinomycin D prevents bortezomib-induced HSF2 mRNA expression, as reflected also at the protein level. Consistently with these observations, actinomycin D treatment prevented bortezomib-induced HSF2 expression also in HeLa cells, both at the RNA and protein levels (Fig. S2A), suggesting an effect of the drug on HSF2 transcription. To verify this hypothesis, newly synthesized (NS) RNA, labeled by adding 5-ethynyl uridine to growing cells and isolated as described in "Materials and methods" section, was analyzed for HSF2 and HSP70 mRNA in MDA-MB-231 cells at different times after bortezomib treatment. As shown in Fig. 3B, bortezomib caused a significant increase in HSF2 NS-RNA at 12 and 24 h after treatment. As expected, high levels of HSP70 NS-RNA were detected in treated samples; it should be noted that, as also shown in Fig. 1D, HSP70 expression is upregulated at an earlier time point than HSF2. A significant

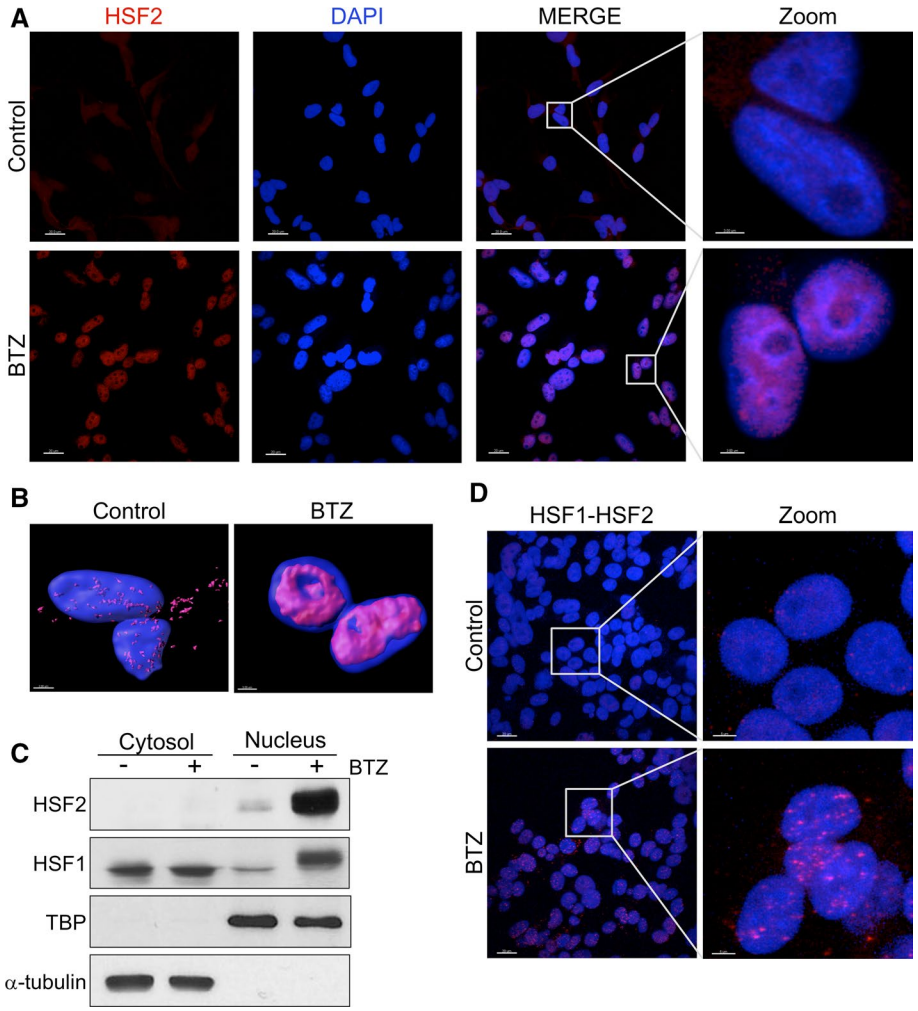

Fig. 2 HSF2 is mainly localized in the nuclei of bortezomib-treated cells and interacts with HSF1. **A** Confocal images of HSF2 (red) intracellular distribution in MDA-MB-231 cells treated with 25 nM bortezomib (BTZ) or vehicle (control) for 14 h. Nuclei were stained with DAPI (blue). Merge images are shown. Scale bar, 20 µm (zoom, 3 µm). **B** Confocal 3D-reconstruction of HSF2 (red) intranuclear localization in MDA-MB-231 cells treated as in **A**. Nuclei were stained with DAPI (blue). Scale bar, 3 µm. The overlay of the fluorochromes is shown. **C** Immunoblot of HSF2 and HSF1 in cytoplasmic and nuclear fractions of MDA-MB-231 cells treated with 25 nM BTZ (+) or vehicle (−) for 14 h. Antibodies against TATA-binding protein (TBP) and α-tubulin were used as a loading control for nuclear and cytoplasmic fractions, respectively. **D** HSF1/HSF2 interactions (visualized as red spots) detected at 14 h after BTZ treatment by in situ proximity ligation assay in MDA-MB-231 cells treated as in **A**. Nuclei are stained with DAPI (blue). Merge and zoom images are shown. Scale bar, 20 µm (zoom, 5 µm)

increase in HSF2 NS-RNA was also found in bortezomib-treated HeLa cells (Fig. 3C). In addition, HSF2 and HSP70 NS-RNAs accumulation was prevented by actinomycin D in bortezomib-treated MDA-MB-231 (Fig. 3D) as well as in HeLa cells (Fig. S2B).

To further investigate whether the bortezomib-induced HSF2 NS-RNA increase was the result of *de novo* gene transcription or the consequence of HSF2 NS-RNA stabilization, an in vitro nuclear *run-on* (NRO) assay was performed on MDA-MB-231 nuclei isolated at different times after bortezomib treatment. A peak of HSF2 and HSP70 NRO-RNA was detected at 12 h after bortezomib treatment (Fig. 3E), demonstrating that the drug regulates HSF2 expression at the transcriptional level. Altogether, these results confirm that bortezomib is able to induce HSF2 transcription in different types of cancer cells.

HSF1 is recruited to the HSF2 promoter during proteasome inhibition

Regulation of HSF2 transcription is still not well understood. Analysis of the human HSF2-promoter nucleotide sequence (JASPAR 2018 database) [56] revealed the presence of two putative HSF1 consensus motifs (HSE), located at 1.397 bp (HSEa) and 1.016 bp (HSEb) upstream of the transcription start site (Fig. 4A, B). As bortezomib triggers HSF1

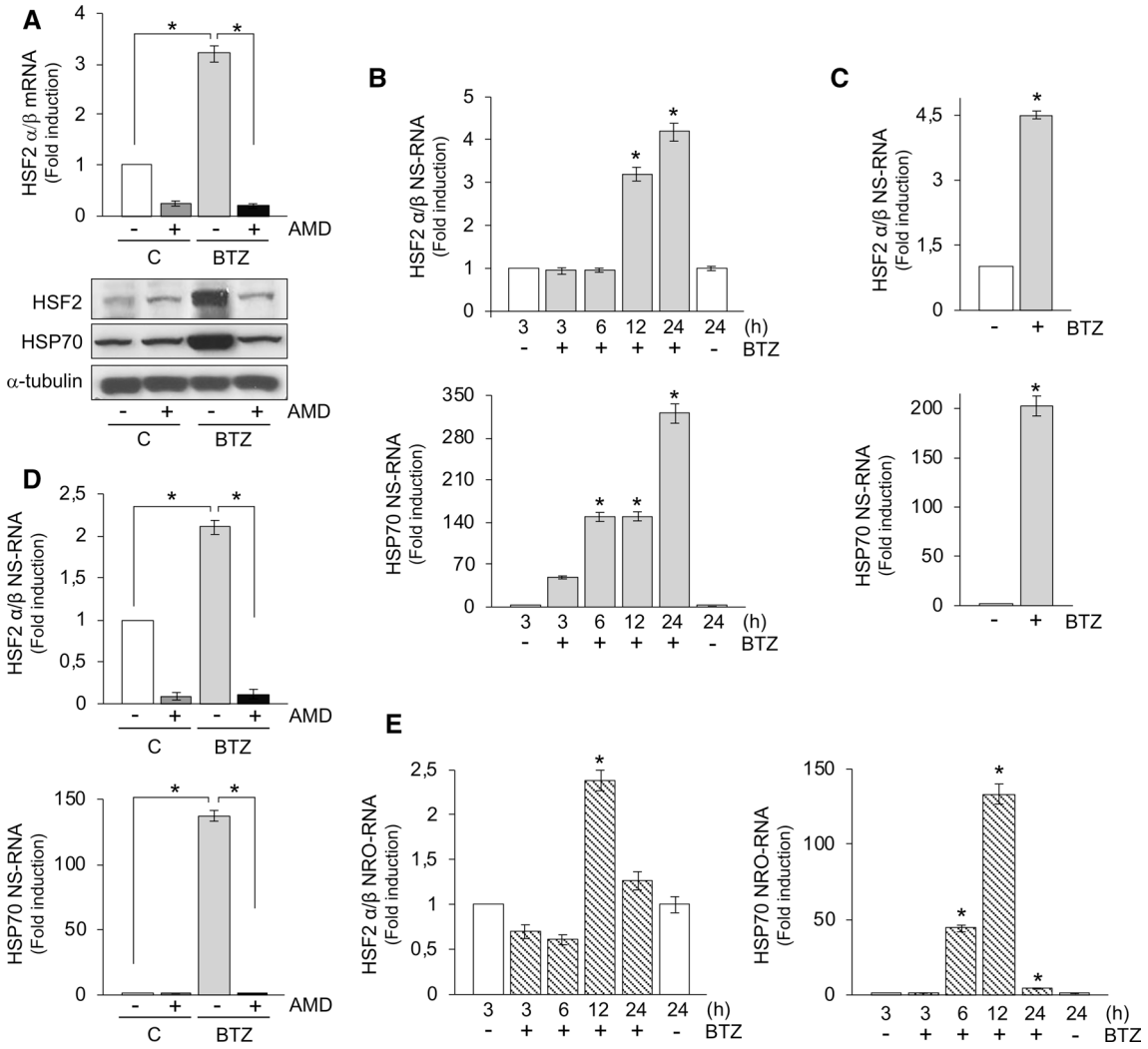

Fig. 3 Bortezomib induces de novo HSF2 transcription in cancer cells. **A** Total RNA of MDA-MB-231 cells treated with 25 nM bortezomib (BTZ) or vehicle (C) for 14 h in the presence (+) or absence (−) of actinomycin D (AMD, 5 µg/ml) was analyzed for HSF2 by qPCR (top panel). In parallel samples, levels of HSF2, HSP70 and α-tubulin were determined by Western blot (bottom panels). **B** Newly synthesized (NS) RNA, isolated by Click-iT Nascent RNA Capture assay, was analyzed for HSF2 and HSP70 by qPCR in MDA-MB-231 cells at different times after treatment with 25 nM BTZ (+). **C** NS-RNA, isolated as in **B**, was analyzed for HSF2 and HSP70 by qPCR in HeLa cells at 14 h after treatment with 25 nM BTZ. **D** NS-RNA isolated in MDA-MB-231 cells treated as in **A** was analyzed for HSF2 and HSP70 by qPCR. **E** Nuclear *run-on* RNA (NRO-RNA) was analyzed for HSF2 and HSP70 in MDA-MB-231 cells treated as in **B** by qPCR. In **A**–**C**, **E**, relative quantities of HSF2 and HSP70 RNAs were normalized to ribosomal L34 RNA levels. Fold increase was calculated by comparing the induction of HSF2 or HSP70 in the treated samples to the relative control (**A**, **C**, **D**) or to control at 3 h (**B**–**E**), which were arbitrarily set to 1. All reactions were made in triplicate using samples derived from at least three biological repeats. Error bars indicate mean ± S.D. ANOVA test (**A**, **B**, **D**, **E**), Student's *t* test (**C**). $*P < 0.05$

activation, the possibility that HSF1 could participate in the bortezomib-mediated regulation of HSF2 expression was investigated.

To this end, MDA-MB-231 cells were treated with bortezomib and, at different times after treatment, WCE were analyzed for HSF1 DNA-binding activity by EMSA, using the ideal HSP70-HSE DNA probe, as well as two DNA probes containing the HSF2-HSEa or the HSF2-HSEb sequences described in Fig. 4B. As shown in Fig. 4C (top), activation of HSF DNA-binding activity

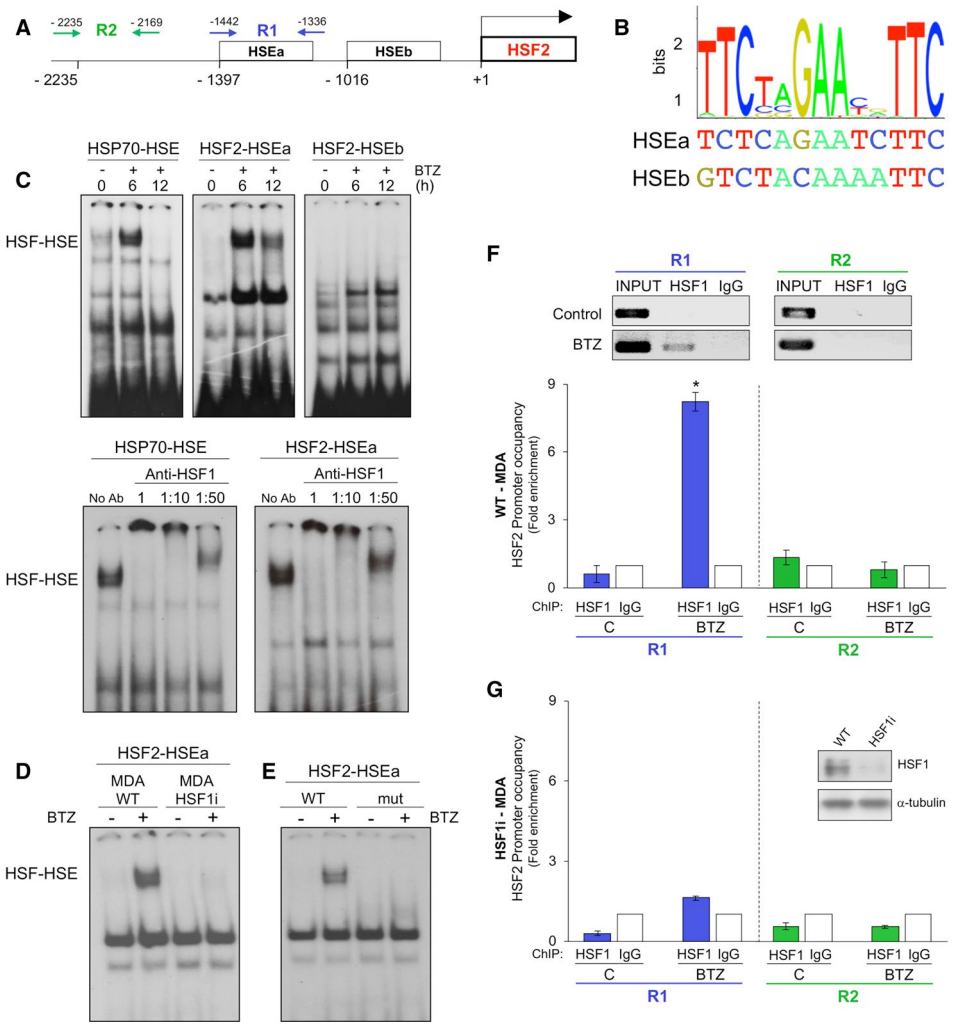

Fig. 4 HSF1 binds directly to the HSF2 promoter. **A** Schematic representation of the human HSF2 promoter. The transcription start site (bent arrow) and putative heat shock elements (HSEa, HSEb) are shown. Arrows indicate locations of the primers (R1, R2) used for ChIP analysis. **B** Sequence logo of the consensus motif for HSF1 generated by the WebLogo program [80] using known HSF1-binding sites (TRANSFAC) [81] (top). Putative HSEa and HSEb sequences identified in the human HSF2 promoter by in silico promoter analysis (JASPAR 2018) [56] are shown (bottom). **C** Analysis of HSF DNA-binding activity in whole-cell extracts (WCE) of MDA-MB-231 cells at different times after 25 nM bortezomib (BTZ, +) treatment by EMSA using an HSP70-HSE ideal probe [50], or two 30-bp DNA fragments containing the HSEa element (from − 1378 to − 1408) or the HSEb element (from − 1000 to − 1030) of the HSF2 promoter region (top panels). WCE from samples treated with BTZ for 6 h were preincubated with different dilutions of anti-HSF1 antibodies and analyzed for supershift assay using the HSP70-HSE and HSF2-HSEa probes (bottom panels). Positions of the HSF DNA-binding complex (HSF-HSE) are shown. **D** Analysis of HSF DNA-binding activity in WCE of wild-type (WT) and HSF1-silenced (HSF1i) MDA-MB-231 cells at 6 h after treatment with 25 nM BTZ (+) or diluent (−) by EMSA using the HSF2-HSEa probe. **E** Analysis of HSF DNA-binding activity in WCE of wild-type MDA-MB-231 cells at 6 h after 25 nM BTZ (+) treatment by EMSA using the HSF2-HSEa probe (WT) or the G-to-T mutated HSF2-HSEa probe (mut) described in Fig. S3B. **F, G** Chromatin from wild-type (WT-MDA, **F**) and HSF1-silenced (HSF1i-MDA, **G**) MDA-MB-231 cells treated with 25 nM BTZ or vehicle (C) for 14 h was immunoprecipitated with anti-HSF1 (HSF1) or anti-IgG (IgG) antibodies. HSF2 promoter regions containing HSEa (R1) and control region (R2) were amplified by PCR in the HSF1 and IgG samples, and in the Input samples (**F**, top panels) and quantified by qPCR (**F**, **G**, bottom panels). HSF1 and α-tubulin protein levels in wild-type (WT) and HSF1-silenced (HSF1i) MDA-MB-231 cells are shown (**G**, inset). In **F**, **G**, fold enrichment was calculated by comparing the enrichment in the HSF1 IP samples to the IgG control, which was arbitrarily set to 1. All reactions were made in triplicate using samples derived from at least three biological repeats. Error bars indicate mean ± SD. Student's *t* test. $^*P < 0.05$

by bortezomib was detected at 6 and 12 h after treatment when the HSP70-HSE and the HSF2-HSEa DNA probes were used; no DNA-binding activity was detected when the HSF2-HSEb probe was used. The specificity of HSF1-DNA binding in HSF1/HSF2-HSEa complexes in bortezomib-treated cells was confirmed by supershift analysis

after preincubation with different dilutions of anti-HSF1 antibodies (Fig. 4C, bottom). No DNA-binding activity was detected in HSF1-silenced MDA-MB-231 cells (Fig. 4D; Fig. S3A); in addition, the insertion of a single mutation (G-to-T, Fig. S3B) in the 5-bp 'nGAAn' unit of the HSEa element resulted in disruption of HSF1 DNA-binding, as analyzed by EMSA (Fig. 4E and Fig. S3C). Taken together these results identify the HSF2-HSEa sequence as a possible HSF1-target in the HSF2 promoter.

The possibility that HSF1 may directly bind to the HSF2 promoter in vivo was then investigated. First, a stably HSF1-silenced MDA-MB-231 cell line (MDA-HSF1i) and a wild-type control cell line (MDA-WT) were generated using RNA-mediated interference as described in "Materials and methods" section. The possibility that HSF1 could be recruited to the HSEa sequence in the HSF2 promoter was analyzed by ChIP assay in MDA-WT and MDA-HSF1i cells treated with 25 nM bortezomib for 14 h. HSF1-coprecipitating DNA was analyzed by PCR and qPCR with primers amplifying two different HSF2 promoter fragments (R1, containing the HSEa sequence, and the negative control R2 fragment, described in Fig. 4A). The specificity of chromatin immunoprecipitation was determined using a control unrelated antibody. A similar analysis was performed in MDA-HSF1i cells, to further verify chromatin immunoprecipitation specificity. An enrichment of the HSEa-containing region (approximately eightfold) was found in bortezomib-treated wild-type cells, whereas no enrichment of control region R2 (that does not contain HSEs) was detected (Fig. 4F); furthermore, no enrichment of the HSEa-containing region was found in HSF1-silenced MDA-MB-231 cells (Fig. 4G).

To verify whether HSF1 recruitment on the HSF2 promoter was dependent on the cell type, a similar study was performed in HeLa cells. To this end, wild-type and stably HSF1-silenced (HSF1i) HeLa cells, described previously [49], were treated with bortezomib and analyzed by ChIP assay. Also in this case an enrichment of the HSEa-containing region was found in wild-type, but not in HSF1i HeLa cells 14 h after bortezomib treatment (Fig. S4A and B). Altogether these results reveal that HSF1 can be recruited to the HSF2 promoter.

Bortezomib-induced HSF2 transcription requires HSF1

The fact that HSF1, following activation by bortezomib treatment, is recruited to the HSF2 promoter in cancer cells, prompted us to investigate the effect of HSF1-silencing on bortezomib-induced HSF2 transcription. In a first set of experiments MDA-MB-231 cells were transiently transfected with two different HSF1-siRNA (siRNA1 and siRNA2) or scramble-RNA. The performance of each of the single siRNAs as well as the pool of two siRNAs was compared to select the best conditions for HSF1-silencing. After 36 h, cells were treated with bortezomib for 14 h, and WCE were analyzed for HSF1, HSF2 and HSP70 levels by Western blot. An efficient HSF1-silencing was obtained with both HSF1-siRNAs and an optimal inhibition was obtained using the pool of siRNA1 and 2, as confirmed also by the lower levels of HSP70 in bortezomib-treated cells (Fig. 5A). Interestingly, HSF1-silencing was found to inhibit bortezomib-induced HSF2 expression.

Next, we analyzed stably HSF1-silenced (MDA-HSF1i) cells as compared to wild-type (MDA-WT) cells at different times after bortezomib treatment. As expected, in HSF1 knockdown cells bortezomib-mediated expression of HSF1 target genes HSP70 and AIRAP was decreased (Fig. 5B, top). Similarly to HSP70 and AIRAP, bortezomib-induced HSF2 expression was also decreased in HSF1 knockdown cells (Fig. 5B, top); in addition, no increase in HSF2 RNA level was detected in HSF1-depleted cells (Fig. 5B, bottom). Finally, analysis of NS-RNA from HSF1 knockdown cells confirmed the absence of HSF2 RNA transcription in bortezomib-treated MDA-HSF1i (Fig. 5B, inset).

To establish whether HSF1 is required for bortezomib-induced HSF2 expression independently of the cell type, HSF1 was stably silenced in different cancer cell lines, including, in addition to MDA-MB-231, HeLa cells, M10 melanoma and MCF7 breast carcinoma cells. Wild-type and HSF1i cells were treated with bortezomib and HSF2 protein and mRNA levels were analyzed at 14 h after treatment. The results confirmed that HSF1-silencing prevents bortezomib-induced HSF2 expression in HeLa cells (Fig. 5C); also in this case, analysis of NS-RNA from HSF1 knockdown cells confirmed the absence of HSF2 RNA transcription in bortezomib-treated HeLa-HSF1i cells (Fig. 5D). Consistently with HSF1i MDA-MB-231 and HeLa cells analysis, HSF1-silencing was found to prevent bortezomib-induced HSF2 expression also in M10 and MCF7 cells as compared to the relative controls (Fig. S5).

Expression of HSF2 in HSF1-depleted cells is rescued by exogenous HSF1 during proteasome inhibition

To further verify the role of HSF1 in bortezomib-induced HSF2 expression, MDA-HSF1i cells were transfected with the Flag-HSF1-pcDNA3 vector expressing the Flag-tagged form of HSF1, or with the empty pcDNA3 vector. After 36 h, cells were treated with bortezomib for 14 h. At this time, WCE were analyzed for levels of HSF2, HSF1, Flag and HSP70 by immunoblot. As shown in Fig. 5E (top panels), HSF1-silencing prevented bortezomib-induced HSF2 expression as expected; however, this effect was markedly

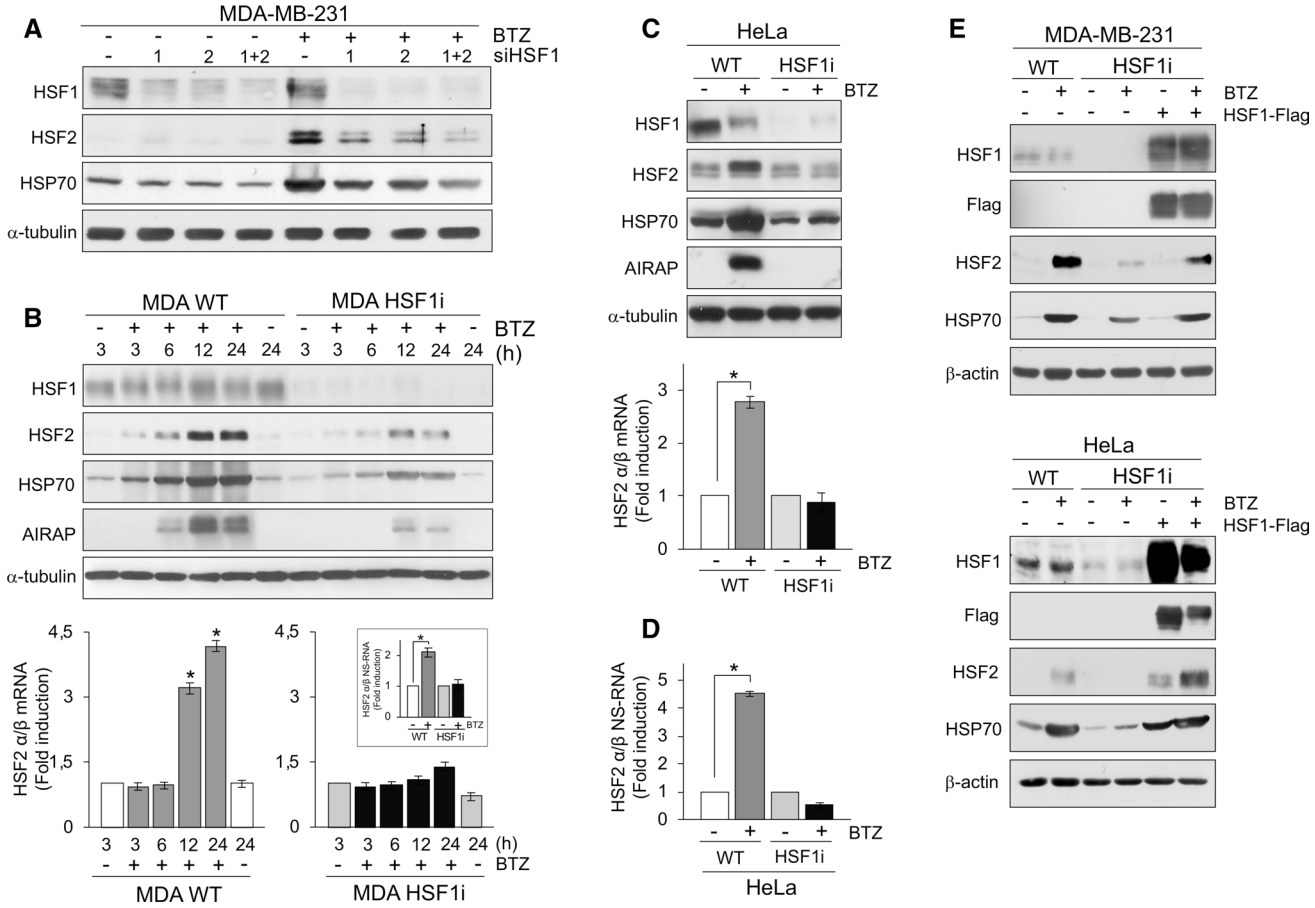

Fig. 5 HSF1 is required for bortezomib-induced HSF2 expression in cancer cells. **A** Immunoblot of HSF1, HSF2, HSP70 and α-tubulin levels in MDA-MB-231 cells transiently transfected with two different HSF1-siRNAs [HSF1-siRNA1 (1) and HSF1-siRNA2 (2)], with the combination of HSF1-siRNA1 and HSF1-siRNA2 (1+2) or with scramble-RNA (−) for 36 h and treated with 25 nM bortezomib (BTZ, +) or vehicle (−) for 14 h. **B** HSF1, HSF2, HSP70, AIRAP and α-tubulin levels determined in whole-cell extracts (WCE) of wild-type (MDA WT) or stably HSF1-silenced (MDA HSF1i) MDA-MB-231 cells at different times after treatment with 25 nM BTZ (+) or vehicle (−) by Western blot (top panels). In parallel, total RNA was analyzed for HSF2 by qPCR (bottom panels). Newly synthesized (NS) RNA, isolated by Click-iT Nascent RNA Capture assay, was analyzed for HSF2 by qPCR in WT and HSF1i MDA-MB-231 cells treated with 25 nM BTZ (+) or vehicle (−) for 14 h (Inset). **C** Immunoblot of HSF1, HSF2, HSP70, AIRAP and α-tubulin levels in WCE of wild-type (WT) and stably HSF1-silenced (HSF1i) HeLa cells treated with 25 nM BTZ (+) or vehicle (−) for 14 h. In parallel, total RNA was analyzed for HSF2 by qPCR. **D** Levels of HSF2 NS-RNA analyzed by qPCR in WT- and HSF1i-HeLa cells treated as in **C**. **E** Western blot analysis of HSF1, Flag, HSF2, HSP70 and β-actin levels in WT and HSF1i MDA-MB-231 cells (top panels) and HeLa cells (bottom panels) transiently transfected with Flag-HSF1-pcDNA3 vector (HSF1-Flag, +) or empty vector (−) for 36 h and treated with 25 nM BTZ (+) or vehicle (−) for 14 h. In **B**–**D**, relative quantities of HSF2 RNA were normalized to ribosomal L34 RNA levels in the same sample. For each cell line, fold increase was calculated by comparing the induction of HSF2 in each sample to the relative control extracted at 3 h (**B**) or 14 h (**B** inset, **C**, **D**), which was arbitrarily set to 1. All reactions were made in triplicate using samples derived from at least five biological repeats. Error bars indicate mean ± S.D. ANOVA test (**B**), Student's *t* test (**B** inset, **C**, **D**). * $P < 0.05$

reduced following exogenous HSF1 overexpression in HSF1-silenced cells, confirming that HSF1 is essential for bortezomib-induced HSF2 transcription in MDA-MB-231 cells. In addition to MDA-MB-231 cells, exogenous HSF1 overexpression was able to rescue the severely impaired HSF2 expression also in HSF1-silenced HeLa cells after bortezomib treatment (Fig. 5E, bottom panels).

Altogether these results demonstrate that HSF1 is critical for HSF2 gene transcription following proteasome inhibition.

HSF2-silencing promotes cancer cell migration

As indicated in "Introduction", differently from HSF1, there is very little information on the role of HSF2 in cancer. Recently, however, HSF2 was implicated in prostate cancer cell invasion [60]. Since MDA-MB-231 cells are known to have a high migratory potential [61], we analyzed the effect of HSF2-silencing on MDA-MB-231 cell migration in the absence or the presence of bortezomib.

MDA-MB-231 cells were transiently transfected with HSF2-siRNA (siHSF2) or scrRNA and, after 36 h, were treated with 25 nM bortezomib (Fig. 6A). At 12 h after treatment, WCE were analyzed for levels of HSF2, HSP70 and PARP, as a marker of apoptosis, by Western blot; in parallel samples, MDA-MB-231 cell viability was determined by vital-dye exclusion assay and cell migration was analyzed by transwell migration assay. Treatment with bortezomib induced the expression of both HSF2 and HSP70 in the scrRNA-transfected cells, as expected (Fig. 6B). Whereas short (12 h) bortezomib treatment did not significantly affect MDA-MB-231 cell viability or PARP cleavage (Fig. 6B, C), the PI was found to markedly decrease MDA-MB-231 cell migration at this time (Fig. 6D, E). HSF2-silencing did not cause a significant change in MDA-MB-231 cell viability, also in the presence of the drug, under the conditions described (Fig. 6B, C). Interestingly, however, HSF2-silencing caused a significant increase in MDA-MB-231 cell migration both in bortezomib-treated and in control cells (Fig. 6D, E), suggesting that HSF2 is involved in regulating the migratory potential in breast cancer cells.

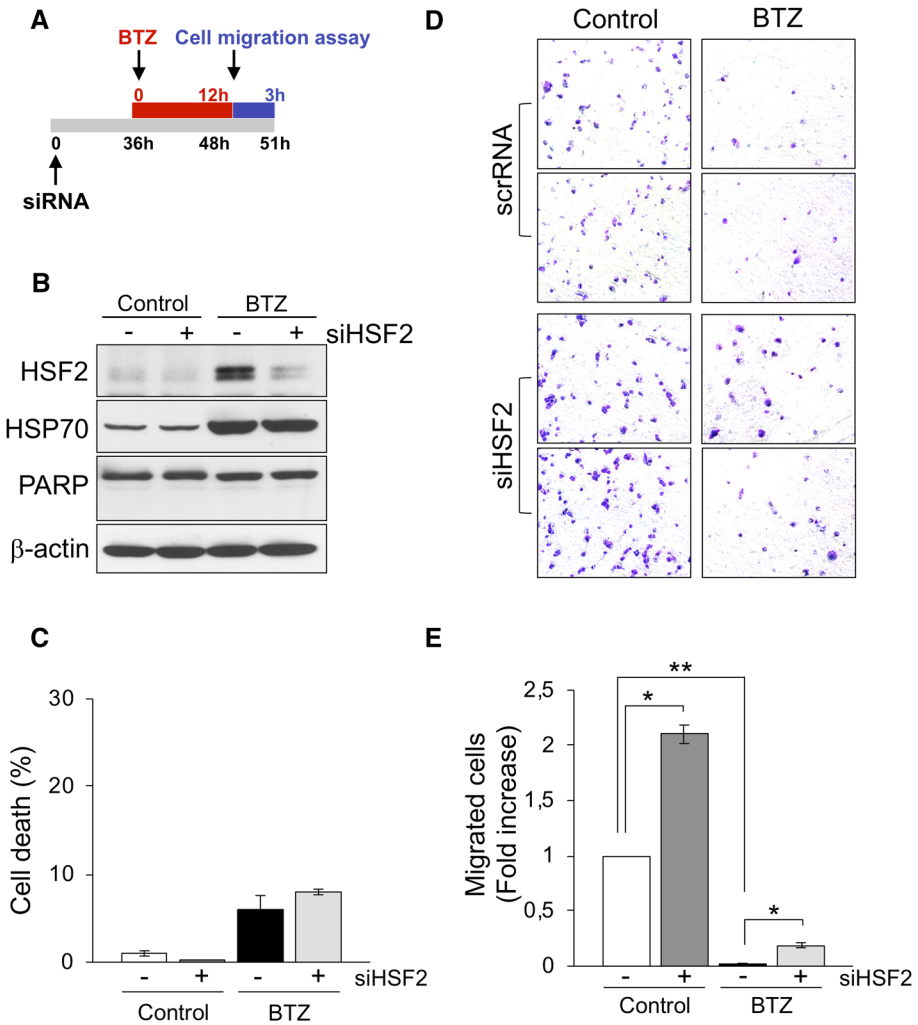

Fig. 6 HSF2-silencing enhances MDA-MB-231 cell migration. **A** Schematic representation of the experimental design. **B** MDA-MB-231 cells were transiently transfected with HSF2-siRNA (siHSF2, +) or scramble-RNA (−), and, after 36 h, were treated with 25 nM bortezomib (BTZ) or vehicle (Control). After 12 h of BTZ treatment, levels of HSF2, HSP70, PARP and β-actin were determined in whole-cell extracts by Western blot. **C** Cell viability was determined by trypan blue staining in parallel samples. **D** Cell migration was analyzed by transwell assay after 12 h of BTZ treatment in cells treated as in **B**. After 3 h, the migratory cells were stained (see "Materials and methods") and photographed using a Leica DM-IL microscope equipped with a 10 × objective, and images were captured on a Leica DC300 camera using Leica-IM500 software. Images shown are representative of four fields per insert. The experiment was made in triplicate. **E** The number of migrated cells in samples described in **D** was counted and expressed as fold increase of the untreated scramble control. In **C**, **E**, data represent the mean ± SD of three replicates. ANOVA test. $*P<0.05$, $**P<0.01$. In **B**, **D**, data from a representative experiment of three biological repeats with similar results are shown

Finally, HSF2-silencing also caused a significant increase in the migration of bortezomib-treated HeLa cells (Fig. S6).

Discussion

HSF1 acts as a guardian of proteome homeostasis in mammalian cells; under proteotoxic stress conditions it orchestrates a cytoprotective response by triggering a rapid shift in the cell transcriptional program resulting in the expression of HSP [14, 15], as well as a broad constellation of target genes encoding proteins with non-chaperone function [23, 25], including proteins implicated in proteasome activity such as ZFAND2A (zinc-finger AN1-type domain-2a) [24]. During the study of ZFAND2A gene regulation by proteasome inhibitors, we came across the interesting observation that bortezomib increased HSF2 mRNA levels in human cells [20]. As indicated in "Introduction", despite the fact that HSF2 is widely recognized as an important factor in embryogenesis and differentiation [31–33], very little is known on HSF2 transcriptional regulation.

We now demonstrate that bortezomib, at clinically relevant concentrations [62], is a potent inducer of HSF2 expression in different types of cancer cells, triggering de novo HSF2 transcription in addition to protein stabilization. Similar results were obtained with the next-generation proteasome inhibitors ixazomib and carfilzomib, indicating that induction of HSF2 expression is a general response to proteasome dysfunction, and prompting us to investigate the mechanism involved. Interestingly, we found that bortezomib-induced HSF2 expression is dependent on the activity of its paralog HSF1. Analysis of the human HSF2 promoter revealed the presence of two putative HSF1 consensus motifs, located at 1.397 bp (HSEa) and 1.016 bp (HSEb) upstream from the transcription start site. HSEa, but not HSEb, was able to bind to HSF1, as shown by electrophoretic mobility shift and supershift assays. Chromatin immunoprecipitation analysis has shown that HSF1 is recruited to the HSEa sequence in the HSF2 promoter after bortezomib treatment in MDA-MB-231 breast cancer cells and in HeLa cells; recruitment was followed by HSF2 transcription in wild-type cells, but not in HSF1-silenced cells. Moreover, reintroduction of the HSF1 gene in HSF1-depleted cells was able to restore inducible HSF2 expression in response to proteasome inhibition. In addition to MDA-MB-231 and HeLa cells, HSF1-silencing prevented bortezomib-induced HSF2 expression in different cancer cell lines, including luminal-like MCF7 breast adenocarcinoma cells and M10 metastatic melanoma cells. Altogether these results demonstrate that HSF1 plays a fundamental role in the control of human HSF2 gene expression during proteasome inhibition.

Since HSF2 expression has not been detected after heat shock despite HSF1 activation [29, 30], we postulate that other factors may contribute to induce HSF1-dependent HSF2 transcription in bortezomib-treated cells, possibly as a consequence of short-lived signaling protein stabilization during proteasome inhibition [63]. The fact that HSF2 itself is stabilized by proteasome inhibitors [30, 41, 51] shares similar DNA-binding domains with HSF1 [22], and it interacts with HSF1 forming heterotrimers [18, 20, 28], suggests that HSF2 could be one of the factors contributing to regulating its own transcription. Electrophoretic mobility supershift assays and ChIP analysis in fact revealed that HSF2 binds to the HSEa sequence, but at a later stage of the proteotoxic stress caused by proteasome dysfunction, concomitant with intranuclear accumulation of the factor (Santopolo et al., personal communication).

In addition to co-factors, changes in local chromatin architecture consequent to PI-induced histone degradation or displacement, as well as in PI-regulated chromatin remodeling enzymes activity [64–66], may be implicated in turning on HSF2 gene transcription, and should be taken into consideration.

Regarding the possible implications of the high levels of HSF2 achieved in cancer cells treated with bortezomib, the fact that drug-induced HSF2 is mostly localized in the nuclei suggests that this transcription factor may participate in bortezomib-regulated transcription in cancer cells, and may thus influence the outcome of the drug treatment.

As indicated in "Introduction", bortezomib is used in the clinic for treatment of multiple myeloma and relapsed mantle cell lymphoma [8], and is known to possess anticancer activity against several other malignancies, including breast cancer [67, 68], based on its direct pro-apoptotic effects on cancer cells as well as its antiangiogenic action [9, 10]. The mechanism of bortezomib anticancer activity is still not completely understood. The initial rationale for its use in cancer treatment was inhibition of nuclear factor-κB (NF-κB) activity by blocking proteasomal degradation of the NF-κB inhibitor IκBα [69]. In addition to NF-κB inhibition, bortezomib was shown to trigger pro-apoptotic factors via activation of the endoplasmic reticulum stress, cause ROS (Reactive Oxygen Species) accumulation, and inhibit angiogenesis; in the case of MM, bortezomib also inhibits MM interaction with bone marrow stromal cells, and regulates the Wnt/β-catenin signaling pathway, by preventing β-catenin protein degradation [70, 71]. On the other hand, bortezomib activates HSF1, and this effect has been associated with cancer cell survival [59] and, in the clinic, with poorer myeloma patient survival [72].

As indicated above, HSF1 protects healthy cells from the damaging effects of proteostasis disruption [43, 73]; cancer cells, due to the need to boost their chaperone system to cope with stress caused by increased protein synthesis, folding, and consequent proteasome overwhelming [43], are more highly dependent on HSF1 than normal cells, presenting a

'non-oncogenic' addiction to HSF1 [15, 74]. In different types of cancers, HSF1 levels and nuclear localization are in fact strongly increased [75–78], and HSF1 was found to regulate a malignant-specific transcriptional program critical for cancer cells and tumor microenvironment [44, 75, 78, 79]. Differently from HSF1, HSF2 has not been extensively investigated in tumor cells, and as indicated above, its function in cancer is largely unknown.

Recently, Bjork et al. [60] have shown that HSF2 acts as a suppressor of prostate cancer cell invasion. We therefore analyzed the effect of HSF2-silencing on the migration of mesenchymal-like breast adenocarcinoma MDA-MB-231 cells, characterized by a high migratory potential [61], and in HeLa cells in the absence or the presence of bortezomib. HSF2 depletion, while it did not significantly affect cell viability under the conditions analyzed (short bortezomib treatment), was found to cause a significant increase in MDA-MB-231 cell migration both in bortezomib-treated and in control cells; HSF2-silencing also promoted cell migration in bortezomib-treated HeLa cells. These results support the hypothesis that HSF2 may regulate the migratory potential of cancer cells, and suggest that this effect may influence bortezomib anticancer activity.

It should also be noted that HSF2 accumulation leads to formation of heterotrimers with HSF1, as shown in MDA-MB-231 and HeLa cells, as well as in other types of cells [18, 20, 28]. The difference in the gene regulatory performance of HSF1 and HSF2 homotrimers *versus* heterocomplexes has not been completely understood. Based on human HSF2 DNA-binding domain structural studies, it was recently suggested that, due to differential wrapping around DNA, HSF1–HSF2 heterotrimers might provide a template for differential and combinatorial regulatory events that would not take place in the case of HSF1 or HSF2 homo-oligomeric complexes [28]. In this regard, it has been reported that HSF1–HSF2 heterotrimers are less efficient than HSF1 homotrimers in activating transcription of several HSF1-target genes [18, 21]; therefore, it could be speculated that, by decreasing the expression of cytoprotective HSF1-target genes, HSF2 may mitigate the prosurvival activity of HSF1 in cancer cells during bortezomib treatment.

Altogether the results provide novel insights into the regulation of HSF2 expression, and reveal an additional level of complexity in the sophisticated interplay between HSF1 and HSF2, representing an interesting example of transcription factors involved in controlling the expression of members of the same family. Because of the important role of HSF2 in development and differentiation, the understanding of the molecular events at the basis of this finely tuned HSF1/HSF2 interplay may lead to advances in the pharmacological modulation of these fundamental transcription factors acting at the crossroads of important physiological and pathological processes in human cells.

Acknowledgments The authors thank G. Zupi (Regina Elena Cancer Institute, Rome, Italy) for providing the M10 melanoma cell line, R. Piva (University of Turin, Italy) for KMM-1 multiple myeloma cells and S. Calderwood (Harvard Medical School, Boston, MA) for the Flag-HSF1-pcDNA3 expression vector. We also thank E. Romano (Center for Advanced Microscopy, University of Rome Tor Vergata) for assistance with confocal microscopy.

Author contributions S.S. performed the study on HSF2 transcription and ChIP analysis; S.S. and A. Rossi performed DNA-binding activity assays; S.S. and A. Riccio performed silencing experiments and analysis of cell survival; A. Riccio and A. Rossi generated stable HSF1-silenced cell lines; S.S. performed the study on cancer cell migration; M.G.S. designed the study; M.G.S. and S.S. wrote the manuscript. All authors contributed to the interpretation of the data and approve the content of the manuscript.

Funding This work was supported by grants from the Italian Ministry of University and Scientific Research (PRIN project N 2010PHT9NF-006).

Compliance with ethical standards

Conflict of interest All authors declare no conflict of interest.

References

1. Labbadia J, Morimoto RI (2015) The biology of proteostasis in aging and disease. Annu Rev Biochem 84:435–464
2. Tomko RJ, Hochstrasser M (2013) Molecular architecture and assembly of the eukaryotic proteasome. Annu Rev Biochem 82:415–445
3. Hershko A, Ciechanover A (1998) The ubiquitin system. Annu Rev Biochem 67:425–479
4. Muratani M, Tansey WP (2003) How the ubiquitin–proteasome system controls transcription. Nat Rev Mol Cell Biol 4:192–201
5. Balch WE, Morimoto RI, Dillin A, Kelly JW (2008) Adapting proteostasis for disease intervention. Science 319:916–919
6. Goldberg AL (2012) Development of proteasome inhibitors as research tools and cancer drugs. J Cell Biol 199:583–588
7. Manasanch EE, Orlowski RZ (2017) Proteasome inhibitors in cancer therapy. Nat Rev Clin Oncol 14:417–433
8. Chen D, Frezza M, Schmitt S, Kanwar J, Dou QP (2011) Bortezomib as the first proteasome inhibitor anticancer drug: current status and future perspectives. Curr Cancer Drug Targets 11:239–253
9. Shahshahan MA, Beckley MN, Jazirehi AR (2011) Potential usage of proteasome inhibitor bortezomib (Velcade, PS-341) in the treatment of metastatic melanoma: basic and clinical aspects. Am J Cancer Res 1:913–924
10. Roccaro AM, Hideshima T, Raje N, Kumar S, Ishitsuka K, Yasui H, Shiraishi N, Ribatti D, Nico B, Vacca A et al (2006) Bortezomib mediates antiangiogenesis in multiple myeloma via direct and indirect effects on endothelial cells. Cancer Res 66:184–191
11. Besse A, Besse L, Kraus M, Mendez-Lopez M, Bader J, Xin BT, de Bruin G, Maurits E, Overkleeft HS, Driessen C (2019) Proteasome inhibition in multiple myeloma: head-to-head comparison of currently available proteasome inhibitors. Cell Chem Biol 26:340–351

12. Akerfelt M, Morimoto RI, Sistonen L (2010) Heat shock factors: integrators of cell stress, development and lifespan. Nat Rev Mol Cell Biol 11:545–555
13. Ritossa F (1962) A new puffing pattern induced by temperature shock and DNP in drosophila. Experientia 18:571–573
14. Lindquist S, Craig EA (1988) The heat-shock proteins. Annu Rev Genet 22:631–677
15. Gomez-Pastor R, Burchfiel ET, Thiele DJ (2018) Regulation of heat shock transcription factors and their roles in physiology and disease. Nat Rev Mol Cell Biol 19:4–19
16. Anckar J, Sistonen L (2011) Regulation of HSF1 function in the heat stress response: implications in aging and disease. Annu Rev Biochem 80:1089–1115
17. Joutsen J, Sistonen L (2019) Tailoring of proteostasis networks with heat shock factors. Cold Spring Harb Perspect Biol. https://doi.org/10.1101/cshperspect.a034066
18. Sandqvist A, Björk JK, Akerfelt M, Chitikova Z, Grichine A, Vourch C, Jolly C, Salminen TA, Nymalm Y, Sistonen L (2009) Heterotrimerization of heat-shock factors 1 and 2 provides a transcriptional switch in response to distinct stimuli. Mol Biol Cell 20:1340–1347
19. Östling P, Björk JK, Roos-Mattjus P, Mezger V, Sistonen L (2007) Heat shock factor 2 (HSF2) contributes to inducible expression of hsp genes through interplay with HSF1. J Biol Chem 282:7077–7086
20. Rossi A, Riccio A, Coccia M, Trotta E, La Frazia S, Santoro MG (2014) The proteasome inhibitor bortezomib is a potent inducer of zinc finger AN1-type domain 2a gene expression: role of heat shock factor 1 (HSF1)–heat shock factor 2 (HSF2) heterocomplexes. J Biol Chem 289:12705–12715
21. Elsing AN, Aspelin C, Björk JK, Bergman HA, Himanen SV, Kallio MJ, Roos-Mattjus P, Sistonen L (2014) Expression of HSF2 decreases in mitosis to enable stress-inducible transcription and cell survival. J Cell Biol 206:735–749
22. Jaeger AM, Makley LN, Gestwicki JE, Thiele DJ (2014) Genomic heat shock element sequences drive cooperative human heat shock factor 1 DNA binding and selectivity. J Biol Chem 289:30459–30469
23. Trinklein ND, Murray JI, Hartman SJ, Botstein D, Myers RM (2004) The role of heat shock transcription factor 1 in the genome-wide regulation of the mammalian heat shock response. Mol Biol Cell 15:1254–1261
24. Rossi A, Trotta E, Brandi R, Arisi I, Coccia M, Santoro MG (2010) AIRAP, a new human heat shock gene regulated by heat shock factor 1. J Biol Chem 285:13607–13615
25. Coccia M, Rossi A, Riccio A, Trotta E, Santoro MG (2017) Human NF-κB repressing factor acts as a stress-regulated switch for ribosomal RNA processing and nucleolar homeostasis surveillance. Proc Natl Acad Sci USA 114:1045–1050
26. Kroeger PE, Morimoto RI (1994) Selection of new HSF1 and HSF2 DNA-binding sites reveals difference in trimer cooperativity. Mol Cell Biol 14:7592–7603
27. Vihervaara A, Sergelius C, Vasara J, Blom MAH, Elsing AN, Roos-Mattjus P, Sistonen L (2013) Transcriptional response to stress in the dynamic chromatin environment of cycling and mitotic cells. Proc Natl Acad Sci USA 110:3388–3397
28. Jaeger AM, Pemble CW IV, Sistonen L, Thiele DJ (2016) Structures of HSF2 reveal mechanisms for differential regulation of human heat-shock factors. Nat Struct Mol Biol 23:147–154
29. Ahlskog JK, Björk JK, Elsing AN, Aspelin C, Kallio M, Roos-Mattjus P, Sistonen L (2010) Anaphase-promoting complex/cyclosome participates in the acute response to protein-damaging stress. Mol Cell Biol 30:5608–5620
30. Mathew A, Mathur SK, Morimoto RI (1998) Heat shock response and protein degradation: regulation of HSF2 by the ubiquitin–proteasome pathway. Mol Cell Biol 18:5091–5098
31. Rallu M, Mt Loones, Lallemand Y, Morimoto R, Morange M, Mezger V (1997) Function and regulation of heat shock factor 2 during mouse embryogenesis. Proc Natl Acad Sci USA 94:2392–2397
32. Pirkkala L, Alastalo TP, Nykanen P, Seppa L, Sistonen L (1999) Differentiation lineage-specific expression of human heat shock transcription factor 2. FASEB J 13:1089–1098
33. Abane R, Mezger V (2010) Roles of heat shock factors in gametogenesis and development. FEBS J 277:4150–4172
34. El Fatimy R, Miozzo F, Le Mouel A, Abane R, Schwendimann L, Saberan-Djoneidi D, de Thonel A, Massaoudi I, Paslaru L, Hashimoto-Torii K et al (2014) Heat shock factor 2 is a stress-responsive mediator of neuronal migration defects in models of fetal alcohol syndrome. EMBO Mol Med 6:1043–1061
35. Kallio M, Chang Y, Manuel M, Alastalo TP, Rallu M, Gitton Y, Pirkkala L, Loones MT, Paslaru L, Larney S et al (2002) Brain abnormalities, defective meiotic chromosome synapsis and female subfertility in HSF2 null mice. EMBO J 21:2591–2601
36. Mou L, Wang Y, Li H, Huang Y, Jiang T, Huang W, Li Z, Chen J, Xie J, Liu Y et al (2013) A dominant-negative mutation of HSF2 associated with idiopathic azoospermia. Hum Genet 132:159–165
37. Akerfelt M, Henriksson E, Laiho A, Vihervaara A, Rautoma K, Kotaja N, Sistonen L (2008) Promoter ChIP-chip analysis in mouse testis reveals Y chromosome occupancy by HSF2. Proc Natl Acad Sci USA 105:11224–11229
38. Wilkerson DC, Murphy LA, Sarge KD (2008) Interaction of HSF1 and HSF2 with the Hspa1b promoter in mouse epididymal spermatozoa. Biol Reprod 79:283–288
39. Sistonen L, Sarge KD, Phillips B, Abravaya K, Morimoto RI (1992) Activation of heat shock factor 2 during hemin-induced differentiation of human erythroleukemia cells. Mol Cell Biol 12:4104–4111
40. Eriksson M, Jokinen E, Sistonen L, Leppa S (2000) Heat shock factor 2 is activated during mouse heart development. Int J Dev Biol 44:471–477
41. Kawazoe Y, Nakai A, Tanabe M, Nagata K (1998) Proteasome inhibition leads to the activation of all members of the heat-shock-factor family. Eur J Biochem 255:356–362
42. Murphy SP, Gorzowski JJ, Sarge KD, Phillips B (1994) Characterization of constitutive HSF2 DNA-binding activity in mouse embryonal carcinoma cells. Mol Cell Biol 14:5309–5317
43. Dai C, Sampson SB (2016) HSF1: guardian of proteostasis in cancer. Trends Cell Biol 26:17–28
44. Mendillo ML, Santagata S, Koeva M, Bell GW, Hu R, Tamimi RM, Fraenkel E, Ince TA, Whitesell L, Lindquist S (2012) HSF1 drives a transcriptional program distinct from heat shock to support highly malignant human cancers. Cell 150:549–562
45. Home T, Jensen RA, Rao R (2015) Heat shock factor 1 in protein homeostasis and oncogenic signal integration. Cancer Res 75:907–912
46. Scomazzon SP, Riccio A, Santopolo S, Lanzilli G, Coccia M, Rossi A, Santoro MG (2019) The zinc-finger AN1-type domain 2a gene acts as a regulator of cell survival in human melanoma: role of E3-ligase cIAP2. Mol Cancer Res. https://doi.org/10.1158/1541-7786.MCR-19-0243
47. Piva R, Gianferretti P, Ciucci A, Taulli R, Belardo G, Santoro MG (2005) 15-Deoxy-$\Delta^{12,14}$-prostaglandin J_2 induces apoptosis in human malignant B cells: an effect associated with inhibition of NF-κB activity and down-regulation of antiapoptotic proteins. Blood 105:1750–1758
48. Wang X, Grammatikakis N, Siganou A, Calderwood SK (2003) Regulation of molecular chaperone gene transcription involves the serine phosphorylation, 14-3-3ε binding, and cytoplasmic sequestration of heat shock factor 1. Mol Cell Biol 23:6013–6026
49. Rossi A, Ciafrè S, Balsamo M, Pierimarchi P, Santoro MG (2006) Targeting the heat shock factor 1 by RNA interference: a potent tool

to enhance hyperthermochemotherapy efficacy in cervical cancer. Cancer Res 66:7678–7685
50. Rossi A, Coccia M, Trotta E, Angelini M, Santoro MG (2012) Regulation of cyclooxygenase-2 expression by heat: a novel aspect of heat shock factor 1 function in human cells. PLoS ONE 7:e31304
51. Rossi A, Elia G, Santoro MG (1997) Inhibition of nuclear factor κB by prostaglandin A_1: an effect associated with heat shock transcription factor activation. Proc Natl Acad Sci USA 94:746–750
52. Mosser DD, Theodorakis NG, Morimoto RI (1988) Coordinate changes in heat shock element-binding activity and HSP70 gene transcription rates in human cells. Mol Cell Biol 8:4736–4744
53. Rossi A, Kapahi P, Natoli G, Takahashi T, Chen Y, Karin M, Santoro MG (2000) Anti-inflammatory cyclopentenone prostaglandins are direct inhibitors of IκB kinase. Nature 403:103–108
54. Rossi A, Elia G, Santoro MG (1998) Activation of the heat shock factor 1 by serine protease inhibitors. An effect associated with nuclear factor-κB inhibition. J Biol Chem 273:16446–16452
55. Roberts TC, Hart JR, Kaikkonen MU, Weinberg MS, Vogt PK, Morris KV (2015) Quantification of nascent transcription by bromouridine immunocapture nuclear run-on RT-qPCR. Nat Protoc 10:1198–1211
56. Khan A, Fornes O, Stigliani A, Gheorghe M, Castro-Mondragon JA, Van Der Lee R, Bessy A, Chèneby J, Kulkarni SR, Tan G et al (2018) JASPAR 2018: update of the open-access database of transcription factor binding profiles and its web framework. Nucleic Acids Res 46:D260–D266
57. Carey MF, Peterson CL, Smale ST (2009) Chromatin immunoprecipitation (ChIP). Cold Spring Harb Protoc. https://doi.org/10.1101/pdb.prot5279
58. Piacentini S, La Frazia S, Riccio A, Pedersen JZ, Topai A, Nicolotti O, Rossignol JF, Santoro MG (2018) Nitazoxanide inhibits paramyxovirus replication by targeting the fusion protein folding: role of glycoprotein-specific thiol oxidoreductase ERp57. Sci Rep 8:10425
59. Shah SP, Lonial S, Boise LH (2015) When cancer fights back: multiple myeloma, proteasome inhibition, and the heat-shock response. Mol Cancer Res 13:1163–1173
60. Björk JK, Åkerfelt M, Joutsen J, Puustinen MC, Cheng F, Sistonen L, Nees M (2015) Heat-shock factor 2 is a suppressor of prostate cancer invasion. Oncogene 35:1770–1784
61. Lehmann BD, Bauer JA, Chen X, Sanders ME, Chakravarthy AB, Shyr Y, Pietenpol JA (2011) Identification of human triple-negative breast cancer subtypes and preclinical models for selection of targeted therapies. J Clin Investig 121:2750–2767
62. Liston DR, Davis M (2017) Clinically relevant concentrations of anticancer drugs: a guide for nonclinical studies. Clin Cancer Res 23:3489–3498
63. Pirkkala L, Alastalo TP, Zuo X, Benjamin IJ, Sistonen L (2000) Disruption of heat shock factor 1 reveals an essential role in the ubiquitin proteolytic pathway. Mol Cell Biol 20:2670–2675
64. Dantuma NP, Groothuis TAM, Salomons FA, Neefjes J (2006) A dynamic ubiquitin equilibrium couples proteasomal activity to chromatin remodeling. J Cell Biol 173:19–26
65. Kikuchi J, Wada T, Shimizu R, Izumi T, Akutsu M, Mitsunaga K, Noborio-Hatano K, Nobuyoshi M, Ozawa K, Kano Y et al (2010) Histone deacetylases are critical targets of bortezomib-induced cytotoxicity in multiple myeloma. Blood 116:406–417
66. Raychaudhuri S, Loew C, Körner R, Pinkert S, Theis M, Hayer-Hartl M, Buchholz F, Hartl FU (2014) Interplay of acetyltransferase EP300 and the proteasome system in regulating heat shock transcription factor 1. Cell 156:975–985
67. Thaler S, Thiede G, Hengstler JG, Schad A, Schmidt M, Sleeman JP (2015) The proteasome inhibitor bortezomib (Velcade) as potential inhibitor of estrogen receptor-positive breast cancer. Int J Cancer 137:686–697
68. Jones MD, Liu JC, Barthel TK, Hussain S, Lovria E, Cheng D, Schoonmaker JA, Mulay S, Ayers DC, Bouxsein ML et al (2010) A proteasome inhibitor, bortezomib, inhibits breast cancer growth and reduces osteolysis by downregulating metastatic genes. Clin Cancer Res 16:4978–4989
69. Palombella VJ, Rando OJ, Goldberg AL, Maniatis T (1994) The ubiquitin–proteasome pathway is required for processing the NF-κB1 precursor protein and the activation of NF-κB. Cell 78:773–785
70. Ri M (2016) Mechanism of action of bortezomib in multiple myeloma therapy. Int J Myeloma 6:1–6
71. Qiang YW, Hu B, Chen Y, Zhong Y, Shi B, Barlogie B, Shaughnessy JD (2009) Bortezomib induces osteoblast differentiation via Wnt-independent activation of β-catenin/TCF signaling. Blood 113:4319–4330
72. Fok JHL, Hedayat S, Zhang L, Aronson LI, Mirabella F, Pawlyn C, Bright MD, Wardell CP, Keats JJ, De Billy E et al (2018) HSF1 is essential for myeloma cell survival and a promising therapeutic target. Clin Cancer Res 24:2395–2407
73. Li J, Labbadia J, Morimoto RI (2017) Rethinking HSF1 in stress, development, and organismal health. Trends Cell Biol 27:895–905
74. Min JN, Huang L, Zimonjic DB, Moskophidis D, Mivechi NF (2007) Selective suppression of lymphomas by functional loss of Hsf1 in a p53-deficient mouse model for spontaneous tumors. Oncogene 26:5086–5097
75. Ciocca DR, Arrigo AP, Calderwood SK (2013) Heat shock proteins and heat shock factor 1 in carcinogenesis and tumor development: an update. Arch Toxicol 87:19–48
76. Chou SD, Murshid A, Eguchi T, Gong J, Calderwood SK (2015) HSF1 regulation of β-catenin in mammary cancer cells through control of HUR/ELAVL1 expression. Oncogene 34:2178–2188
77. Su KH, Cao J, Tang Z, Dai S, He Y, Sampson SB, Benjamin IJ, Dai C (2016) HSF1 critically attunes proteotoxic-stress sensing by mTORC1 to combat stress and promote growth. Nat Cell Biol 18:527–539
78. Santagata S, Hu R, Lin NU, Mendillo ML, Collins LC, Hankinson SE, Schnitt SJ, Whitesell L, Tamimi RM, Lindquist S et al (2011) High levels of nuclear heat-shock factor 1 (HSF1) are associated with poor prognosis in breast cancer. Proc Natl Acad Sci USA 108:18378–18383
79. Kourtis N, Moubarak RS, Aranda-Orgilles B, Lui K, Aydin IT, Trimarchi T, Darvishian F, Salvaggio C, Zhong J, Bhatt K et al (2015) FBXW7 modulates cellular stress response and metastatic potential via HSF1 post-translational modification. Nat Cell Biol 17:322–332
80. Crooks GE, Hon G, Chandonia JM, Brenner SE (2004) WebLogo: a sequence logo generator. Genome Res 14:1188–1190
81. Heinemeyer T, Wingender E, Reuter I, Hermjakob H, Kel AE, Kel OV, Ignatieva EV, Ananko EA, Podkolodnaya OA, Kolpakov FA et al (1998) Databases on transcriptional regulation: TRANSFAC, TRRD and COMPEL. Nucleic Acids Res 26:362–367